

Embedding any desired number of coexisting attractors in memristive system

Chunbiao Li(李春彪), Ran Wang(王然), Xu Ma(马旭), Yicheng Jiang(姜易成), and Zuohua Liu(刘作华)
Citation: Chin. Phys. B, 2021, 30 (**12**): 120511. DOI: 10.1088/1674-1056/ac1e1f
Journal homepage: http://cpb.iphy.ac.cn; http://iopscience.iop.org/cpb

What follows is a list of articles you may be interested in

Dynamic modeling and aperiodically intermittent strategy for adaptive finite-time synchronization control of the multi-weighted complex transportation networks with multiple delays

Ning Li(李宁), Haiyi Sun(孙海义), Xin Jing(靖新), and Zhongtang Chen(陈仲堂)
Chin. Phys. B, 2021, 30 (**9**): 090507. DOI: 10.1088/1674-1056/abea92

Nonlinear vibration of iced cable under wind excitation using three-degree-of-freedom model

Wei Zhang(张伟), Ming-Yuan Li(李明远), Qi-Liang Wu(吴启亮), and An Xi(袭安)
Chin. Phys. B, 2021, 30 (**9**): 090503. DOI: 10.1088/1674-1056/abea83

Generating multi-layer nested chaotic attractor and its FPGA implementation

Xuenan Peng(彭雪楠), Yicheng Zeng(曾以成), Mengjiao Wang(王梦蛟), and Zhijun Li(李志军)
Chin. Phys. B, 2021, 30 (**6**): 060509. DOI: 10.1088/1674-1056/abda34

Linear synchronization and circuit implementation of chaotic system with complete amplitude control

Chun-Biao Li(李春彪), Wesley Joo-Chen Thio, Julien Clinton Sprott, Ruo-Xun Zhang(张若洵), Tian-Ai Lu(陆天爱)
Chin. Phys. B, 2017, 26 (**12**): 120501. DOI: 10.1088/1674-1056/26/12/120501

Multi-scroll hidden attractors and multi-wing hidden attractors in a 5-dimensional memristive system

Xiaoyu Hu(胡晓宇), Chongxin Liu(刘崇新), Ling Liu(刘凌), Yapeng Yao(姚亚鹏), Guangchao Zheng(郑广超)
Chin. Phys. B, 2017, 26 (**11**): 110502. DOI: 10.1088/1674-1056/26/11/110502

SPECIAL TOPIC — Interdisciplinary physics: Complex network dynamics and emerging technologies

Embedding any desired number of coexisting attractors in memristive system*

Chunbiao Li(李春彪)[1,2,†], Ran Wang(王然)[1,2], Xu Ma(马旭)[1,2], Yicheng Jiang(姜易成)[1,2], and Zuohua Liu(刘作华)[3]

[1] *Jiangsu Collaborative Innovation Center of Atmospheric Environment and Equipment Technology (CICAEET), Nanjing University of Information Science & Technology, Nanjing* 210044, *China*

[2] *School of Artificial Intelligence, Nanjing University of Information Science & Technology, Nanjing* 210044, *China*

[3] *State Key Laboratory of Coal Mine Disaster Dynamics and Control, Chongqing University, Chongqing* 400044, *China*

(Received 10 July 2021; revised manuscript received 5 August 2021; accepted manuscript online 17 August 2021)

A simple variable-boostable system is selected as the structure for hosting an arbitrarily defined memristor for chaos producing. The derived three-dimensional (3-D) memristive chaotic system shows its distinct property of offset, amplitude and frequency control. Owing its merits any desired number of coexisting attractors are embedded by means of attractor doubling and self-reproducing based on function-oriented offset boosting. In this circumstance two classes of control gates are found: one determines the number of coexisting attractors resorting to the independent offset controller while the other is the initial condition selecting any one of them. Circuit simulation gives a consistent output with theoretically predicted embedded attractors.

Keywords: offset boosting, attractor doubling, attractor self-reproducing, memristive system

PACS: 05.45.–a, 05.45.Ac, 05.45.Pq **DOI:** 10.1088/1674-1056/ac1e1f

1. Introduction

Memristor is regarded as a new component for circuit design, which has a specific voltage–current restriction with fingerprint characteristics of 8-like pinched hysteresis loop.[1–5] Because of the nonlinear feature, memristor brings chaos possibility even in a very simple system.[6–13] As a memory component, the dynamical states in its networks can characterize various patterns in information system. Coexisting attractors controlled by a direct switch or simple hardware configuration could be helpful for state representation and conducive to the integration of storage and calculation. As a result, it is valuable to explore the dynamics of a simple memristive node and control its states for information processing.

Multistability in memristive systems has been exhaustedly explored, among which extreme multistability[14–20] and coexistence with infinitely many attractors[21–24] seem especially striking. In the area of information engineering, the number of coexisting attractors seems to be an important issue for effective information representation or signal acquisition. For memristive chaos-based application, there are two challenges lying in this direction, one of which is to find a simple structure for hosting a memristor to give offset boostable chaos while the other one aims to get its attractor controlled by a single knob or hardware configuration. If we ignore the real products of memristors and model a freely defined memristor with representative inherent fingerprints, such a three-dimensional (3-D) memristive system is thereby not far away from our goal. In fact, people can investigate those existing systems and try to find the distinct memristor variable dependence. Following with a further nonlinear reforming, a fresh 3-D memristive system is derived for embedding coexisting attractors, as shown in Fig. 1.

Offset control is the fundamental principle for attractor doubling[25–27] and attractor self-reproducing.[28–30] By introducing multiple piecewise-like functions into a seed system, the dominant dynamics generally finds its way for attractor self-reproducing. It was pointed that the substitution of a proper absolute value function gives robust attractor doubling in the routine of symmetrization while the periodic function repeats the desired dynamics in a direct easy way for attractor self-reproducing. Attractor-doubling represents a direct double multiplication while the attractor self-reproducing is helpful for direct cumulative counting. Two regimes of attractor embedding could be applied for effective information representation or even numerical calculating. For a memristive system, system-based attractor doubling and self-reproducing preserve the fundamental system dynamics without changing the architecture and memristor component. The new born attractors stand by in system space as desired depending on the attached function substitutions and provide broad possibilities for information processing in some way.

*Project supported by the National Natural Science Foundation of China (Grant Nos. 61871230 and 51974045) and the Natural Science Foundation of Jiangsu Province, China (Grant No. BK20181410).

†Corresponding author. E-mail: goontry@126.com, chunbiaolee@nuist.edu.cn

© 2021 Chinese Physical Society and IOP Publishing Ltd

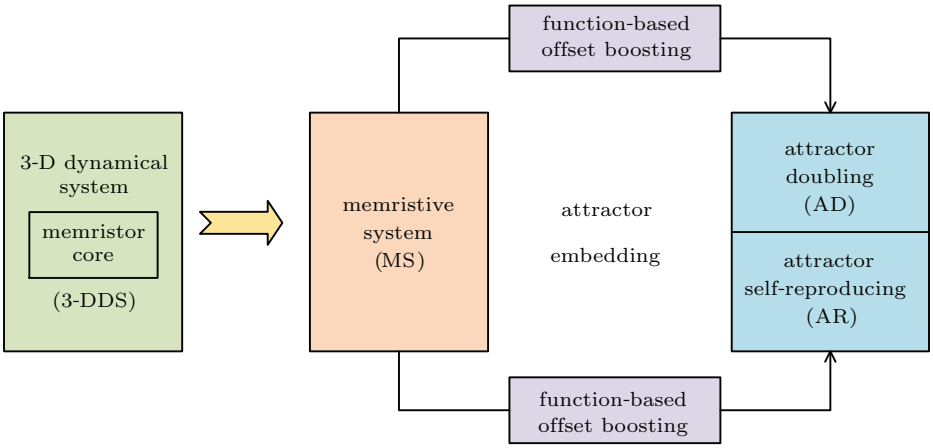


Fig. 1. Nonlinearly reforming for embedding any number of coexisting attractors.

In this work, any number of coexisting attractors in a 3-D memristive system are obtained from a very direct offset-based processing. In Section 2, a simple 3-D memristive system is derived from an existing variable boostable system.[31] In Section 3, any number of coexisting attractors are embedded into the derived memristive system in the dimension of system variable with two different regimes: attractor doubling and attractor self-reproducing. The former provides a direct multiplication control while the latter resorts to the combination of signum and periodic function. In Section 4, circuit simulation is completed for physical verification. In fact, coexisting attractors stand in phase space can be recognized by an exact initial condition. Corresponding discussion is wrapped in the last section.

2. A unique offset-boostable 3-D memristive system

It is found that system (1) (VB6)[31] could be reformed to host a memristor, which gives chaos as system (2),

$$\begin{cases} \dot{x} = 1 - yz, \\ \dot{y} = az^2 - yz, \\ \dot{z} = x, \end{cases} \tag{1}$$

$$\begin{cases} \dot{x} = c - (b\,|y| - 1)z, \\ \dot{y} = az^2 - yz, \\ \dot{z} = x, \end{cases} \tag{2}$$

where the following memristor is introduced in the first dimension:

$$\begin{cases} i = W(y)z, \\ W(y) = b\,|y| - 1, \\ \dot{y} = az^2 - yz. \end{cases} \tag{3}$$

When $a = 0.6$, the memductance and pinched hysteresis loop are plotted in Fig. 2. Here the variable y is regarded as the internal variable and the introduced memristor has piecewise linear memductance.

When $a = 0.6$, $b = 1$, and $c = 1$, memristive system (2) shows chaotic oscillation with Lyapunov exponents $(0.1793, 0, -1.1809)$ and Kaplan–Yorke dimension $D_{\mathrm{KY}} = 2.1518$ under initial condition $(-1, 1, -1)$, as shown in Fig. 3. Note that the internal variable y and system variables x and z all exhibit chaotic oscillation.

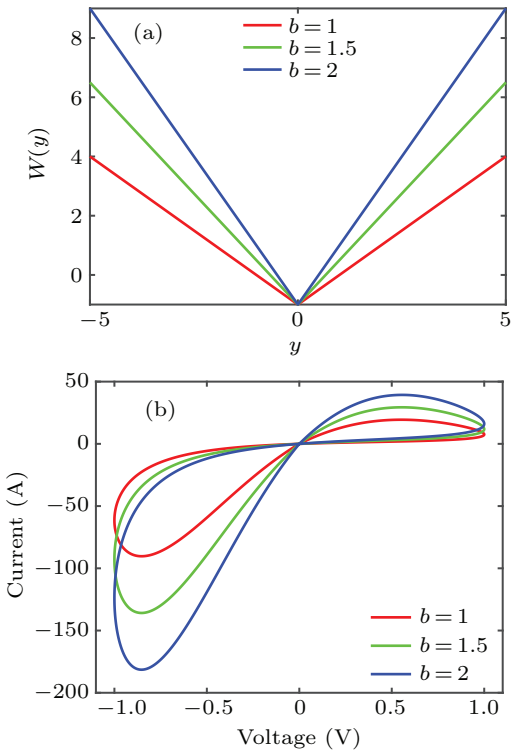


Fig. 2. The memductance and pinched hysteresis loop with sinusoidal excitation under $f = 0.1$: (a) memductance, (b) pinched hysteresis.

System (2) is offset boostable, which can be proved with a direct substitution like $x \to x + m$. Moreover, in the specifically introduced memristor the inherent property of voltage-current relation is determined by the two parameters a and b. It turns out that the parameter b rescales the amplitude of system variable x negatively while the frequency proportionally

in a limited region as shown in Fig. 4, which has never been reported in other memristive systems. The evolvement of amplitude and frequency can be seen directly from the waveform and frequency spectra, as shown in Fig. 5. To understand the function of parameter b, here take a substitution

$$x \to m^2 x, \quad y \to my, \quad z \to mz, \quad t \to t/m, \tag{4}$$

we can see that both the second and third dimensions of system (2) remain unchanged while the first dimension turns to be $\dot{x} = \frac{c}{m^3} - (\frac{b}{m}|y| - \frac{1}{m^2})z(m > 0)$. For relatively large m, $\dot{x} \approx -(\frac{b}{m}|y|)z$, and therefore the integrated parameter b rescales the variables x, y, z and t closing to the restriction according to Eq. (4).

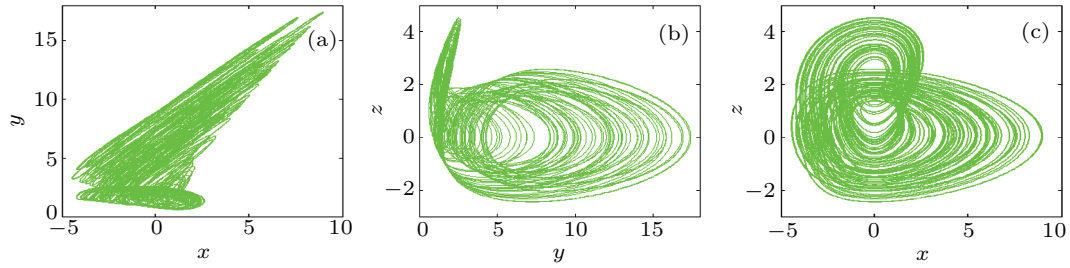


Fig. 3. Chaotic attractor in system (2) with $a = 0.6$, $b = 1$, $c = 1$, and initial condition $(-1, 1, -1)$: (a) x–y, (b) y–z, (c) x–z.

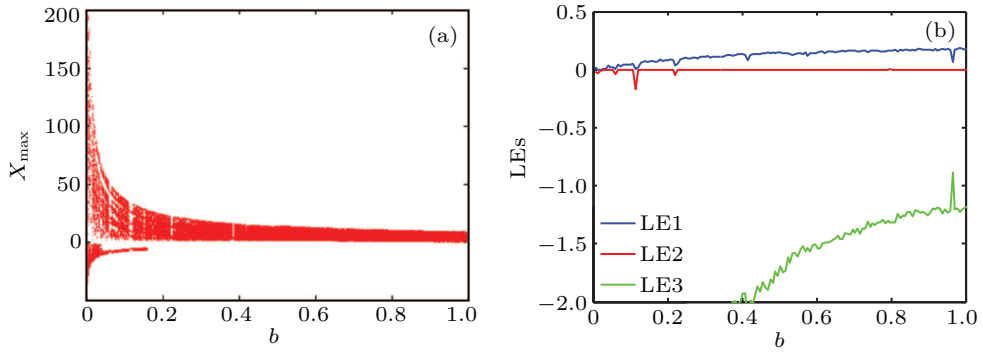


Fig. 4. Dynamical evolvement of system (2) with $a = 0.6$, $c = 1$, IC $= (-1, 1, -1)$: (a) bifurcation behavior, (b) Lyapunov exponents.

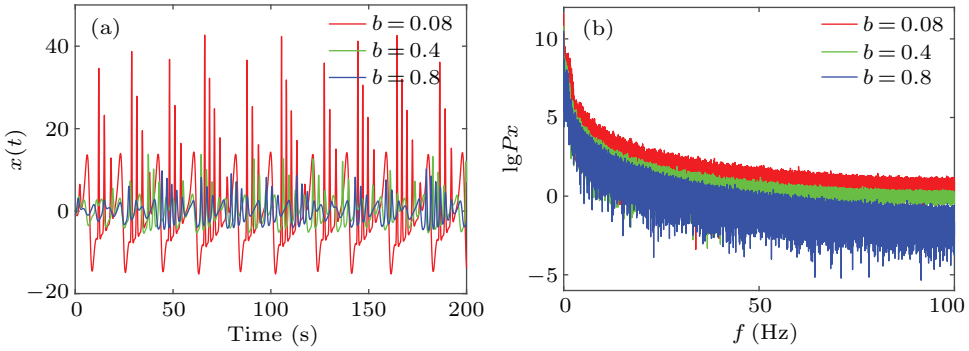


Fig. 5. Chaotic oscillation of system (2) with $a = 0.6$, $c = 1$, IC $= (-1, 1, -1)$: (a) chaotic signal $x(t)$, (b) frequency spectrum.

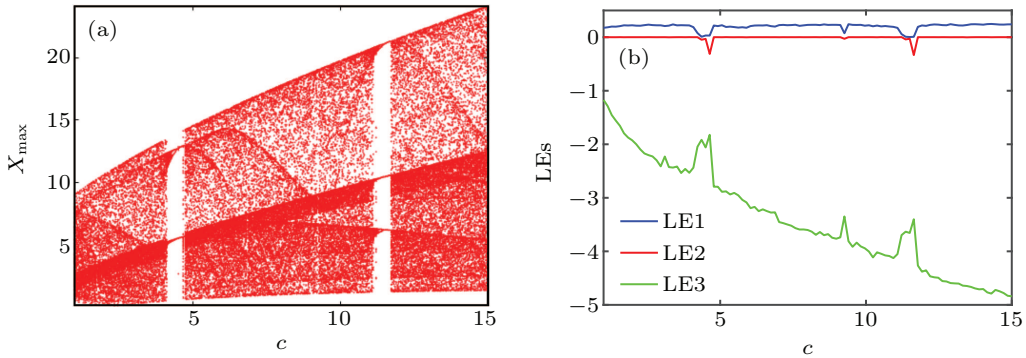


Fig. 6. Dynamics of system (2) with $a = 0.6$, $b = 1$, IC $= (-1, 1, -1)$: (a) bifurcation diagram, (b) Lyapunov exponents.

Moreover, system (2) exhibits robust chaos according to the parameter c, which also rescales the amplitude of system variable x in a quasilinear way with occasionally inserted periodic windows, as shown in Fig. 6. When c increases in region $[0, 15]$, only a couple of periodic oscillations break in triggering the collapse of the Lyapunov exponents. All the above analysis shows that system (2) is unique in terms of parameter sensitivity. Two parameters, namely, system parameter c and memristor parameter b both show their independent function of amplitude control. Memristor parameter b also brings time rescaling for Lyapunov exponent modification.

3. Two regimes of attractor embedding

The coexisting attractors can be controlled by function-based offset boosting. However, one is resort to attractor doubling, and the other is resort to attractor self-reproducing. Therefore, these two approaches bring coexisting attractors with different scales. Attractor doubling can be used to simulate the key processing for high bit generation in binary number representation while attractor self-reproducing can be applied for representation of numerical accumulation. Attractor doubling introduces more parameters for attractor embedding and resorts to system modification more violently. These parameters form control gates by which the number of coexisting attractors is determined by the series[32] if coexisting attractors are doubled more than one times. Attractor self-reproducing seems easier for embedding more attractors even more to infinity. But this seems to out of control if not sufficient control gates are planted. In fact, in both routines of attractor embedding, sufficient offset gates are necessary for controlling the number of coexisting attractors. Only by this, any one of the embedded attractors can be visited by a selected initial condition gate accordingly.

3.1. Attractor doubling

The direct substitution of the absolute value function can make the coexisting attractors doubled. The single linear term x in the third dimension of system (2) makes the dimension x easily offset boostable, leaving a convenient conversion for attractor doubling. Substituting x with $|x| - d$ as

$$\begin{cases} \dot{x} = \mathrm{sgn}(x)(c - (b|y| - 1)z), \\ \dot{y} = az^2 - yz, \\ \dot{z} = |x| - d. \end{cases} \tag{5}$$

The doubled attractors are controlled with desired distance by the control gate of d. Note that small gate d makes the coexisting attractors be linked together forming pseudo-double-scroll. Then a pseudo-double-scroll attractor is captured when coexisting attractors get linked together because of the connected basins of attraction. The doubled coexisting attractors stand in phase space in the dimension of x, as shown in Fig. 7. As a result, the derived system (5) now turns to be a symmetrical system hatching coexisting symmetrical pairs of attractors or pseudo-multiple-scroll attractors.

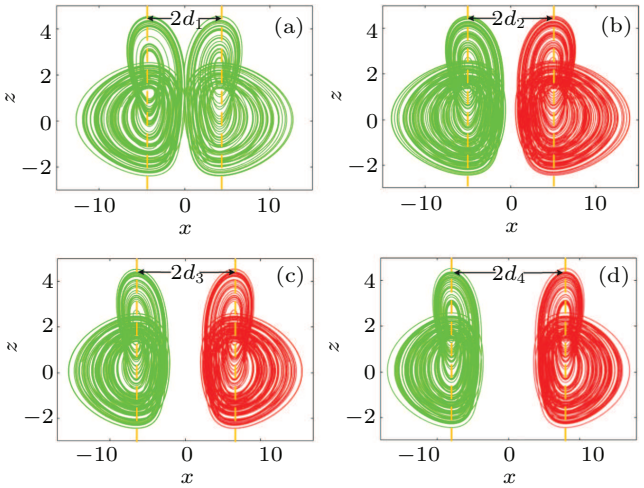


Fig. 7. Embedded attractors in system (5) with $a = 0.6$, $b = 1$, $c = 1$ under various control gates. IC $= (1, 1, -1)$ is red and IC $= (-1, 1, -1)$ is green:(a) $d_1 = 4.11$ (pseudo-double-scroll attractor), (b) $d_2 = 5$, (c) $d_3 = 6.5$, (d) $d_4 = 8$ (double coexisting attractors).

Furthermore, this operation can be repeated in the dimension z, but this will destroy the feedback of the originally introduced memristor. For doubling the attractors according to the dimension of z, the derivative of internal variable turns to be associated with the absolute function with offset gate e, and the following equation is obtained:

$$\begin{cases} \dot{x} = c - (b|y| - 1)(|z| - e), \\ \dot{y} = a(|z| - e)^2 - y(|z| - e), \\ \dot{z} = \mathrm{sgn}(z)x. \end{cases} \tag{6}$$

The substitution of z with $|z| - e$ changes the original system more drastically. Doubled attractors locate in the dimension of z as predicted, as shown in Fig. 8. Since the system variable is more controllable than the memristor, this transformation does not bring too much trouble since the derivative of y comes from the feedback of y and the flexible function of system variable z even though we see that this transformation does not fully utilize the property of easy offset boosting.

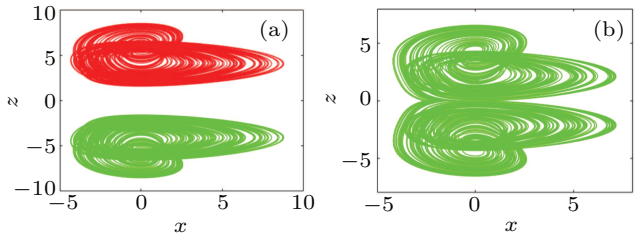


Fig. 8. Coexisting attractors in system (6) with $a = 0.6$, $b = 1$, $c = 1$, IC $= (-1, 1, 1)$ is red and IC $= (-1, 1, -1)$ is green: (a) a symmetric pair of coexisting attractors under control gate $e = 4$, (b) pseudo-double-scroll attractor under control gate $e = 2.05$.

Doubling coexisting attractors can also be executed in both dimensions of x–z, where two control gates d and e are

necessary for settling any of the attractors to desired position as in the following equation:

$$\begin{cases} \dot{x} = \mathrm{sgn}(x)(c - (b|y| - 1)(|z| - e)), \\ \dot{y} = a(|z| - e)^2 - y(|z| - e), \\ \dot{z} = \mathrm{sgn}(z)(|x| - d). \end{cases} \tag{7}$$

Smaller control gate d makes coexisting attractors link together in the dimension of x forming two pseudo-two-scroll attractors, while combined small control gate e puts the doubled pseudo-two-scroll attractors together forming a pseudo-four-scroll attractor, as shown in Fig. 9. Corresponding signal waveforms are plotted in Fig. 10. Note that two control gates should be arranged with two newly introduced signum functions. The process of attractor doubling depends on the revise of the system structure. Two signum functions $\mathrm{sgn}(x)$, $\mathrm{sgn}(z)$ and two control gates d, e in two absolute value functions embed at most four coexisting attractors. For more attractors, the substitution of the absolute value function needs to be repeated, bringing more control gates and switching functions.[32] However, attractor embedding can turn to another way, where the property of offset boosting can be used for more convenient attractor embedding. In the following, we discuss how to embed any desired number of attractors by introducing a periodic function.

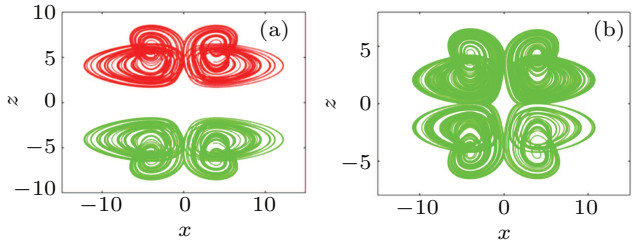


Fig. 9. Embedded attractors in system (7) with $a = 0.6$, $b = 1$, $c = 1$, IC $= (-1, 1, 1)$ is red and IC $= (-1, 1, -1)$ is green: (a) a symmetric pair of coexisting pseudo-two-scroll attractors under control gates $d = 4$, $e = 4$, (b) pseudo-four-scroll attractor under $d = 4$, $e = 2$.

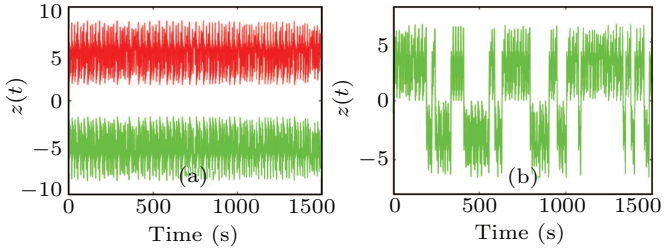


Fig. 10. Waveform of coexisting oscillations in system (7) with $a = 0.6$, $b = 1$, $c = 1$, IC $= (-1, 1, 1)$ is red and IC $= (-1, 1, -1)$ is green: (a) $d = 4$, $e = 4$ (coexisting pseudo-two-scroll attractors), (b) $d = 4$, $e = 2$ (pseudo-four-scroll attractor).

3.2. Attractor self-reproducing

The above attractor embedding has a discrete scale, where the number of coexisting attractors depends on the times of absolute-value-function substitution. Each operation needs an extra function introducing. In fact, infinitely many attractors are available by introducing a periodic trigonometric function to the offset boostable variable. Based on this, further control for embedding any number of coexisting attractors is resort to the modification of the periodic function. Applying signum function, the number of coexisting attractors can be controlled by newly introduced offset gate. Memristive system (2) has a single system variable x in the right hand, and can be modified as

$$\begin{cases} \dot{x} = c - (b|y| - 1)z, \\ \dot{y} = az^2 - yz, \\ \dot{z} = F(x). \end{cases} \tag{8}$$

When $F(x) = 1.25\sin(0.2x)(\mathrm{sgn}(x) + 1)(\mathrm{sgn}(-x + d) + 1)$, coexisting attractors can be controlled by the offset gate of d. Comparing with the approach based on system (4) (with one absolute value function and one signum function) and system (7) (with two absolute value functions and two signum functions), here in system (8), a sinusoidal function modified by two signum functions provides a free control of any coexisting attractors. The principle can be clearly indicated by the curve of the control function shown in Fig. 11. Here the control gate d selects the number of coexisting attractors. Positive d outputs coexisting attractors in positive direction and vice versa. As shown in Fig. 12, a couple of coexisting attractors are controlled by control gates d. If we want to select coexisting attractors in desired region, two independent control gates d should be set according to the two signum functions. More control gates pose more precise and flexible control. Mixed control can be obtained if an extra substitution of the absolute value function in the dimension of z is made, and correspondingly the selected attractors will get doubled in the z dimension. One can do this for his convenience. Control gate d should be selected according to the size of an attractor.

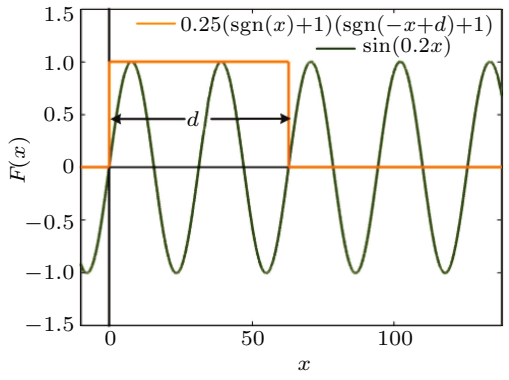


Fig. 11. The curve of the control function for attractor embedding.

Furthermore, the function $F(x)$ can be replaced by a piecewise linear function and other trigonometric functions. For example, tangent function can be applied into system (8) for hatching coexisting attractors according to its period. When $F(x) = 72\tan(0.05x)$, infinitely many coexisting attractors are born distributing in phase space with interval of

20π between any of two attractors. Applying more control gates based on signum function, more than that, embedded coexisting attractors can be edited in a more flexible way. For example, when $F(x) = 1.25\sin(0.2x)(\mathrm{sgn}(x)+1)(\mathrm{sgn}(-x+d_1)+1)+4.5\tan(0.05x)(\mathrm{sgn}(x-d_2)+1)(\mathrm{sgn}(-x+d_3)+1)$, embedded attractors are edited in region of $[0,d_1]$ with interval of 10π and $[d_2,d_3]$ with interval of 20π, as shown in Fig. 13. Coexisting attractors can be selected and edited by choosing any combination of periodic trigonometric function and signum function. Control gate leaves a convenient channel for attractor group selection while initial condition gate realizes the precise positioning of a desired attractor. However, the control gate has priority over the initial condition.

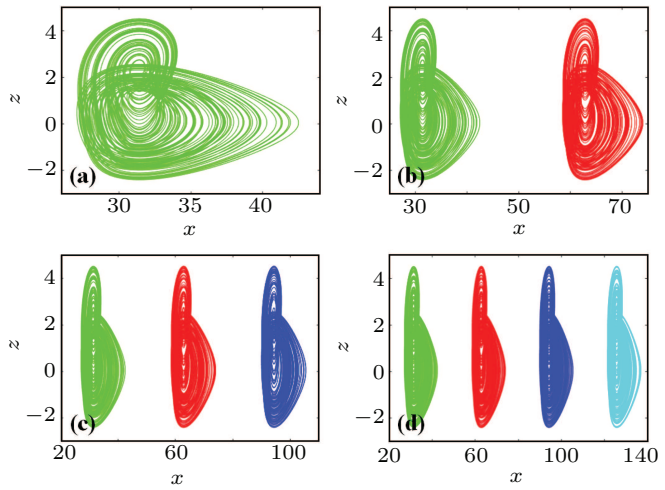


Fig. 12. Embedded coexisting attractors in system (8) with $F(x) = 1.25\sin(0.2x)(\mathrm{sgn}(x)+1)(\mathrm{sgn}(-x+d)+1)$, $a = 0.6$, $b = 1$, $c = 1$, IC $= (1+10\pi, 1, -1)$ is green, IC $= (1+20\pi, 1, -1)$ is red, IC $= (1+30\pi, 1, -1)$ is blue and IC $= (1+40\pi, 1, -1)$ is cyan: (a) $d = 12+10\pi$, (b) $d = 12+20\pi$, (c) $d = 12+30\pi$, (d) $d = 12+40\pi$.

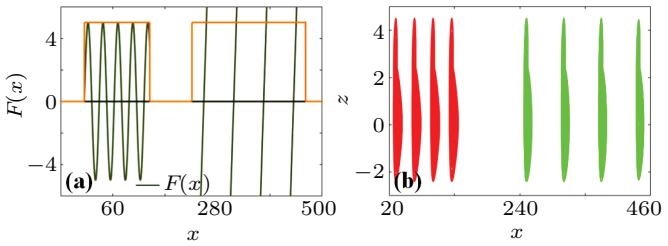


Fig. 13. Control function and embedded coexisting attractors in system (8) with $F(x) = 1.25\sin(0.2x)(\mathrm{sgn}(x)+1)(\mathrm{sgn}(-x+d_1)+1)+4.5\tan(0.05x)(\mathrm{sgn}(x-d_2)+1)(\mathrm{sgn}(-x+d_3)+1)$, $d_1 = 12+40\pi$, $d_2 = -25+80\pi$, $d_3 = 25+140\pi$, $a = 0.6$, $b = 1$, $c = 1$, IC $= (1+10\pi/20\pi/30\pi/40\pi, 1, -1)$ are red, IC $= (1+80\pi/100\pi/120\pi/140\pi, 1, -1)$ are green: (a) control function, (b) embedded attractors.

4. Circuit implementation

To verify the above system design for attractor embedding, circuit-based experiment is realized for further observation. To realize system (2), a memristor simulator is designed in Fig. 14. Here the derivative of internal variable y is connected with system variable z. Therefore system (5) for attractor doubling turns to be

$$\begin{cases} \dot{x} = \dfrac{1}{R_1C_1}\mathrm{sgn}(x) - \dfrac{1}{R_2C_1}W(y)z\cdot\mathrm{sgn}(x), \\ \dot{z} = \dfrac{1}{R_3C_2}|x| - V_1. \end{cases} \tag{9}$$

Circuit modules associated with the absolute value function are constructed for attractor doubling. According to the parameters combined with a time scale for attractor showing in oscilloscope, circuit parameters are selected in Fig. 15 as $C_1 = C_2 = C_3 = 10$ nF, $R_1 = R_2 = R_3 = R_4 = R_{10} = R_{23} = R_{31} = R_{32} = R_{33} = 10$ kΩ, $R_5 = R_6 = R_7 = R_8 = R_{11} = R_{12} = R_{13} = R_{14} = R_{15} = R_{16} = R_{17} = R_{18} = R_{19} = R_{20} = R_{21} = R_{24} = R_{25} = R_{26} = R_{27} = R_{28} = R_{29} = R_{30} = 100$ kΩ, $R_9 = 140$ kΩ, $R_{22} = 16.67$ kΩ, $V_2 = 1$ V. Like the attractors plotted in Fig. 7, the pseudo-double-scroll attractor and coexisting attractors are captured as shown in Fig. 16.

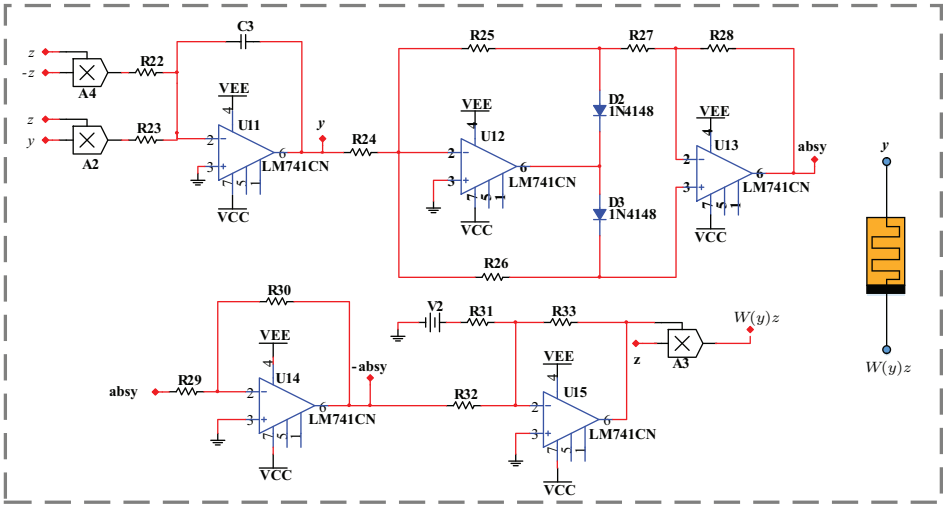


Fig. 14. The analog equivalent circuit schematic of memristor (3).

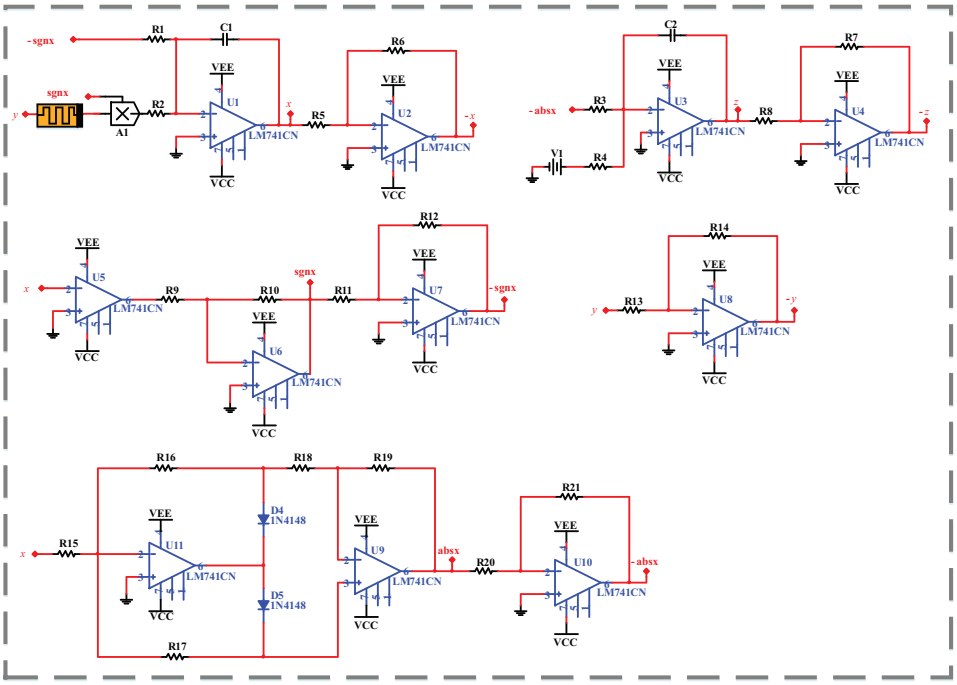


Fig. 15. Circuit schematic of memristive system (5).

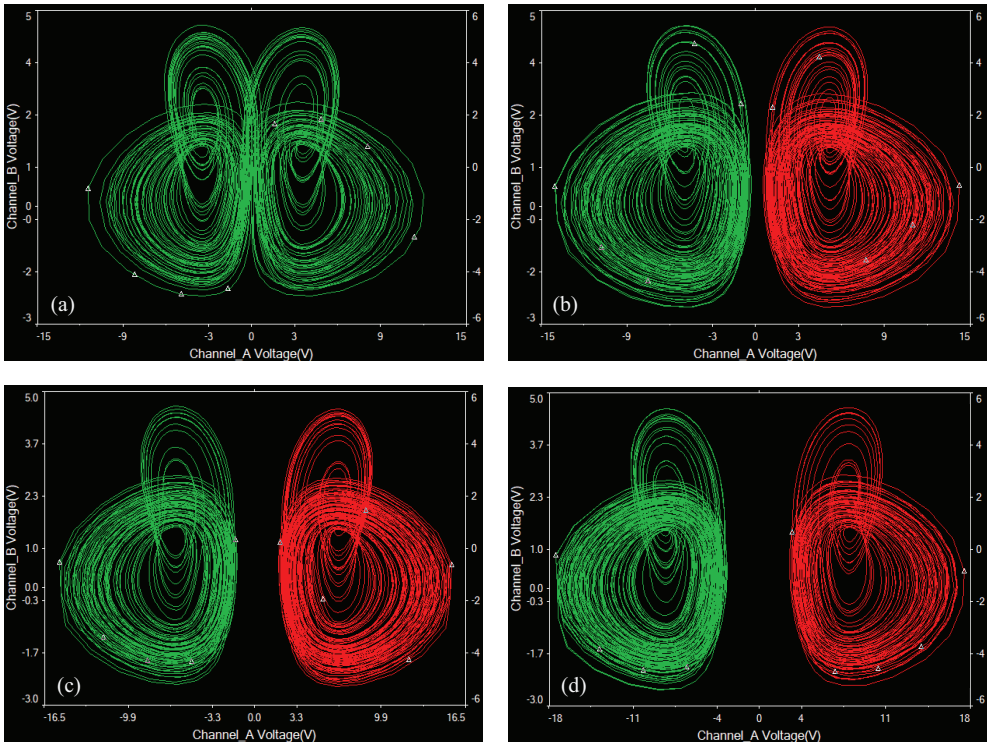


Fig. 16. Coexisting attractors in system (5) with $V_1 = 1$ V, IC $= (1, 1, -1)$ is red and IC $= (-1, 1, -1)$ is green: (a) pseudo-double-scroll attractor under $V_1 = 4.11$ V, (b)–(d) a symmetric pair of coexisting attractors under $V_1 = 5$ V, $V_1 = 6.5$ V, and $V_1 = 8$ V.

For doubling coexisting attractors in the dimensions of x and z, more modules are applied for absolute value function realization, the revised system (7) turns to be the circuit with the following equation:

$$\begin{cases} \dot{x} = \dfrac{1}{R_1 C_1}\operatorname{sgn}(x) - \dfrac{1}{R_2 C_1} W(y)(|z| - V_3)\operatorname{sgn}(x), \\ \dot{z} = \dfrac{1}{R_3 C_2}\operatorname{sgn}(z)\,|x| - \dfrac{1}{R_4 C_2}\operatorname{sgn}(z). \end{cases} \tag{10}$$

To realize system (10), a memristor simulator is designed in Fig. 17. According to the parameters combined with a time scale for attractor showing in oscilloscope, circuit components in Fig. 18 are $C_1 = C_2 = C_3 = 10$ nF, $R_1 = R_2 = R_3 = R_{10} = R_{23} = R_{31} = R_{32} = R_{33} = R_{34} = R_{35} = R_{36} = R_{37} = R_{38} = R_{47} = 10$ kΩ, $R_5 = R_6 = R_7 = R_8 = R_{11} = R_{12} = R_{13} = R_{14} = R_{15} = R_{16} = R_{17} = R_{18} = R_{19} = R_{20} = R_{21} = R_{24} = R_{25} = R_{26} = R_{27} = R_{28} = R_{29} = R_{30} = R_{39} = R_{40} = R_{41} = R_{42} = R_{43} = R_{44} = R_{45} = R_{48} = R_{49} = 100$ kΩ, $R_4 = 2.5$ kΩ, $R_9 = R_{46} = 140$ kΩ, $R_{22} = 16.67$ kΩ, $V_2 = 1$ V. Like the embedded attractors and waveform of oscillations plotted in Figs. 9 and 10, the pseudo-double-scroll attractor, pseudo-four-scroll and waveform of oscillations are captured as shown in Fig. 19.

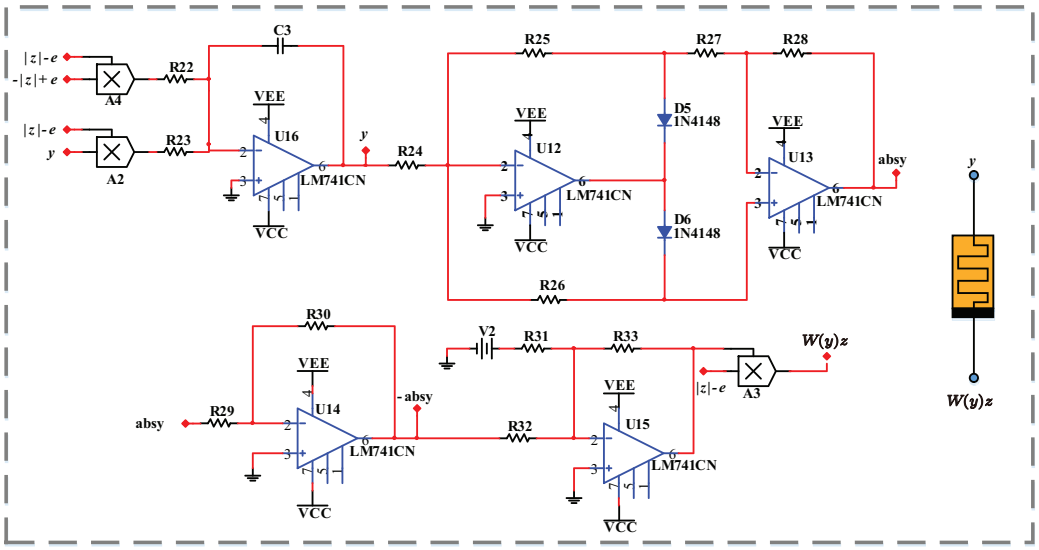


Fig. 17. The analog equivalent circuit schematic of the memristor.

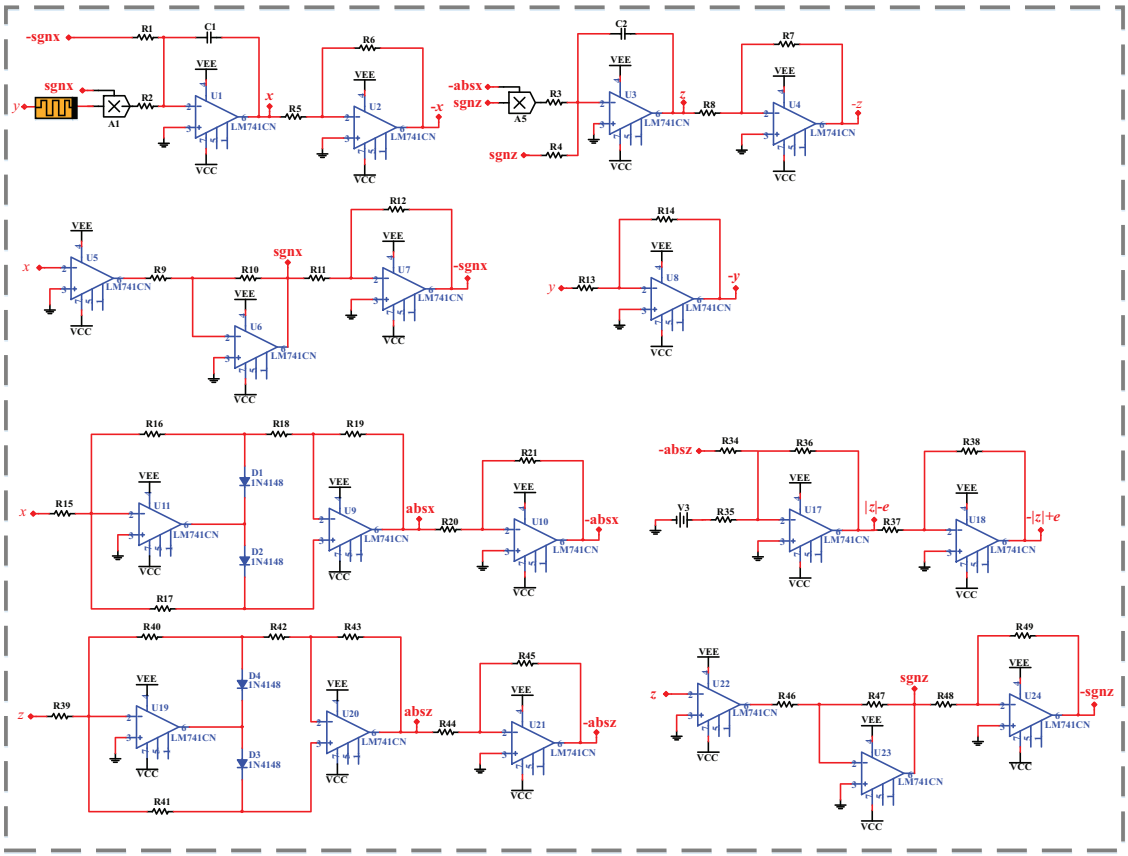


Fig. 18. Circuit schematic of memristive system (7).

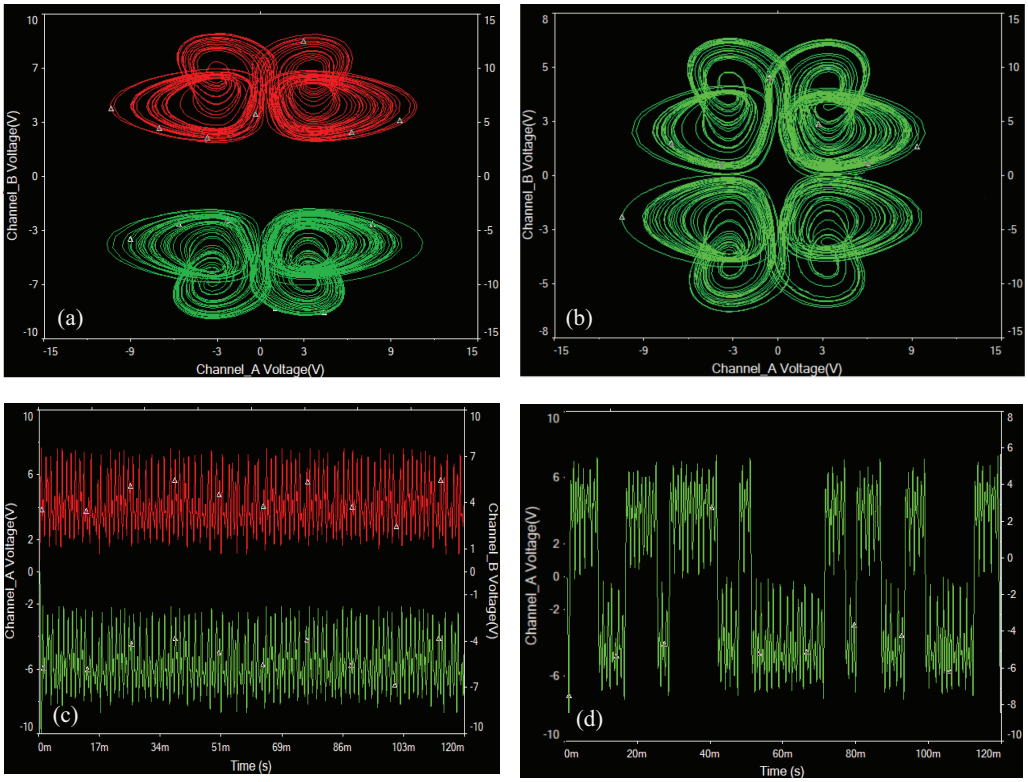


Fig. 19. Attractors and chaotic signals in circuit (10) with $V_2 = 1$ V, IC $= (-1, 1, 1)$ is red and IC $= (-1, 1, -1)$ is green: (a) a symmetric pair of coexisting pseudo-double-scroll attractors with $V_3 = 4$ V, (b) pseudo-four-scroll attractor with $V_3 = 2$ V, (c) a symmetric pair of chaotic signals under $V_3 = 4$ V, (d) chaotic signal under $V_3 = 2$ V.

5. Discussion and conclusion

Flexible memristor definition can make great contribution for constructing a 3-D chaotic memristive system, where additional nonlinearity typically does not destroy the fundamental dynamics inherited from the seed system. In fact, we can construct more 3-D chaotic systems from the existing 3-D manifolds or by defining more mathematical models of memristor. Memristor introducing in a variable-boostable system brings more convenience for attractor embedding. In this work, from the view of attractor embedding, a simple 3-D memristive system is derived, in which the basic property of variable boosting is not destroyed. It brings great convenience for attractor doubling. Besides this, periodic trigonometric function substitution makes the attractor self-reproducing in the dimension of offset boostable variable more conveniently. A simple absolute value function substitution combined with a switch function realizes attractor doubling. Doubling coexisting attractors depends on the operation of function substitution in which the absolute value function determines the intervals and signum function provides necessary polarity balance. Absolute value functions and other periodic trigonometric functions can be applied for attractor embedding with any number of coexisting attractors. There is an obstacle standing in the way of attractor doubling, which is how to realize the substitution of the absolute function in a simple replicable way. Periodic trigonometric function combined with signum function provides an easy way for attractor embedding and control. Further work aiming to this direction is expected in the near future.

References

[1] Chua L O 1971 *IEEE Trans. Circuit Theory* **18** 507
[2] Chua L O and Kang S M 1976 *Proc. IEEE* **64** 209
[3] Chua L O 2014 *Semiconductor Science Technology* **29** 104001
[4] Adhikari S P, Sah M P, Kim H and Chua L O 2013 *IEEE Trans. Circuits Syst. I* **60** 3008
[5] Peng Y X, Sun K H and He S B 2020 *Chaos, Solitons & Fractals* **137** 109873
[6] Qin C, Sun K H and He S B 2021 *Electronics* **10** 841
[7] Lai Q, Wan Z Q, Kuate P D K and Fotsin H 2020 *Communications in Nonlinear Science and Numerical Simulation* **89** 105341
[8] Peng Y X, He S B and Sun K H 2021 *Results in Physics* **24** 104106
[9] Zhang X H, Wu Z Z and Chua L O 2020 *Inter. J. Bifurcat. Chaos* **30** 2030023
[10] Ruan J Y, Sun K H, Mou J, He S B and zhang L M 2018 *Euro. Phys. J. Plus* **133** 3
[11] Peng Y X, He S B and Sun K H 2020 *AEU - International Journal of Electronics and Communications* **129** 153539
[12] Wan Q Z, Zhou Z T, Ji W K, Wang C H and Yu F 2020 *Complexity* **1** 1
[13] Cheng Y Z, Min F H, Rui Z and Zhang L 2021 *Chin. Phys. B*
[14] Chang H, Li Y X, Chen G R and Yuan F 2020 *Inter. J. Bifurcat. Chaos* **30** 434
[15] Li Z J, Zhou C Y and Wang M J 2019 *AEU - International Journal of Electronics and Communications* **100** 127
[16] Yuan F, Wang G Y and Wang X W 2016 *Chaos* **26** 507
[17] Li C, Min F H, Jin Q S and Ma H Y 2017 *AIP Adv.* **7** 125204
[18] Lin H R, Wang C H and Tan Y M 2020 *Nonlinear Dyn.* **99** 2369

[19] Chang H, Li Y X, Yuan F and Chen G R 2019 *Inter. J. Bifurcat. Chaos* **29** 1950086

[20] Zhang Y Z, Liu Z, Wu H G, Chen S Y and Bao B C 2019 *Euro. Phys. J. Spec. Top.* **228** 1995

[21] Lai Q, Wan Z Q, Kengne L K, Kamdem Kuate P D and Chen C Y 2021 *IEEE Trans. Circuits Syst. II* **68** 2197

[22] Jin Q S, Min F H and Li C B 2019 *Chin. J. Phys.* **62** 342

[23] Gu J C, Li C B, Chen Y D, Herbert I U and Lei T F 2020 *IEEE Access* **8** 12394

[24] Bao H, Hua Z Y, Li H Z, Chen M and Bao B C 2021 *IEEE Trans. Circuits Syst. I* **99** 1

[25] Li C B, Sprott J C, Liu Y J, Gu Z Y and Zhang J W 2018 *Inter. J. Bifurcat. Chaos* **28** 1850163

[26] Li C B, Sun J Y, Lu T A and Lei T F 2020 *Symmetry* **12** 574

[27] Gu Z Y, Li C B, Pei X F, Tao C Y and Liu Z H 2020 *Euro. Phys. J. Spec. Top.* **229** 1007

[28] Li C B, Sun J Y, Lu T A, Sprott J C and Liu Z H 2020 *Chaos* **30** 063144

[29] Sun J Y, Li C B, Lu T A, Akgul A and Min F H 2020 *IEEE Access* **2** 139289

[30] Kong S X, Li C B, Jiang H B, Lai Q and Jiang X W 2021 *Chaos* **31** 043121

[31] Li C B and Sprott J C 2016 *Optik* **127** 10389

[32] Li C B, Lu T A, Chen G R and Xing H Y 2019 *Chaos* **29** 51102